SHARP INTERFACE LIMITS OF THE CAHN–HILLIARD EQUATION WITH DEGENERATE MOBILITY

ALPHA ALBERT LEE , ANDREAS MÜNCH , AND ENDRE SÜLI *

Abstract. We consider the sharp interface limit of the degenerate Cahn–Hilliard equation with polynomial free energy via matched asymptotic analysis involving exponentially growing terms and multiple inner layers. With a quadratic mobility, a contribution from nonlinear, porous-medium type bulk diffusion to the normal flux condition for the interface motion appears in the limit model to the same order as surface diffusion. Moreover, the contribution can be either one or two-sided depending on the initial condition for the phase field variable. For higher degeneracy, bulk diffusion does not enter to leading order, so that in the limit the normal velocity is proportional to the surface Laplacian of the mean curvature of the interface, as required for surface diffusion. The resulting sharp interface models are corroborated by comparing relaxation rates for an axisymmetric stationary state perturbed by azimuthal perturbations with numerically obtained values for the phase field model. This work clarifies some confusion in the current literature as to when degenerate Cahn–Hilliard equations can be used for numerical methods designed to solve the surface diffusion free boundary problem.

1. Introduction. Phase field models are a common framework to describe the mesoscale kinetics of phase separation and pattern-forming processes [58, 23]. Since phase field models replace a sharp interface by a diffuse order parameter profile, they avoid numerical interface tracking, and are versatile enough to capture topological changes. Although models can be constructed starting from a systematic coarse-graining of the microscopic Hamiltonian [35, 34, 33, 32], the use as a numerical tool to solve free boundary problems requires careful consideration of their correct asymptotic long-time sharp interface limits are. These limits must reliably approach the behaviour of the free boundary problem.

One of the simplest and most common models that describes phase separation in a binary system for a conserved order parameter, u, is the Cahn–Hilliard equation [55],

$$u_t = -\nabla \cdot \mathbf{j}, \qquad \mathbf{j} = -M(u)\nabla\mu \qquad \mu = -\varepsilon^2\nabla^2 u + f'(u). \tag{1.1}$$

with constant mobility and a biquadratic form for the homogeneous free energy, respectively,

$$M(u) = M_0(u) \equiv 1, \qquad f(u) = f_p(u) \equiv (u^2-1)^2/2. \tag{1.2}$$

The Cahn–Hilliard equation (1.1) has been written here as a system using the flux $\mathbf{j}$ and the chemical potential μ; the "gradient coefficient" ε measures the width of the interface layer. The sharp interface limit $\varepsilon \to 0$ for this case has been shown by Pego [57] (and subsequently proven rigorously by Alikakos et al. [2]) to reduce to the so-called Mullins–Sekerka problem [54] on a long time scale $t = O(\varepsilon^{-1})$. Richer interface dynamics with, for example, kinetic undercooling and different diffusivity in the two pure phases, can be obtained as the sharp interface limits of more complex phase field models with coupled order parameters (see e.g. references [41, 42, 3]).

The system (1.1) with constant mobility and biquadratic homogeneous free energy can be seen as an approximation of the Cahn–Hilliard equation with a concentration-

*Mathematical Institute, University of Oxford, Andrew Wiles Building, Woodstock Road, Oxford, OX2 6GG

dependent mobility and a logarithmic free energy [55, 47],

$$M(u) = 1 - u^2, \tag{1.3a}$$

$$f(u) = f_l(u) \equiv \frac{1}{2}\theta\left[(1+u)\ln(1+u) + (1-u)\ln(1-u)\right] + \frac{1}{2}(1-u^2), \tag{1.3b}$$

in the shallow quench limit, $\theta \to 1$, where θ is the temperature. The concentration dependent mobility and the difference between f_l and f_p become important in particular for $\theta \to 0$. A concentration dependent mobility appears naturally in the original derivation of the Cahn–Hilliard equation, see [18], and the form above is a thermodynamically reasonable choice [19, 63]. The logarithmic terms in the homogeneous free energy f_l arise from entropic contributions and the last term is an enthalpy term for the molecular interactions [21], see also [32, 45, 59, 14] for other approaches and related models. The sharp interface asymptotics for Cahn–Hilliard equations with degenerate mobility is more subtle than for the constant mobility case. Cahn et al. [20] considered the deep quench limit, $\theta = 0$, and for $\varepsilon \to 0$ found that (1.1), (1.3) reduce to a model for surface diffusion, where the normal velocity of the interface is proportional to the surface Laplacian of the mean curvature. Heuristically, the degeneracy of the mobility function at the pure phases suppresses the mass flux in the normal direction and therefore the diffusion from or into the bulk.

Despite (1.3) being well-motivated physically (see the previously cited literature), other combinations of free energy and mobility have been used in the literature for the phase separation of polymer mixtures [69, 68], and as a basis in particular for numerical approaches to surface diffusion [22], often in more complex situations with additional physical effects, such as the electromigration in metals [53], heteroepitaxial growth [60], anisotropy [64, 65] or e.g. in solid-solid dewetting [40] and coupled to fluid flow [1, 62]. Often, a biquadratic double-well free energy such as f_p is combined with the mobility M_1 or with the doubly degenerate mobility $M_2(u) = (1-u^2)^2$. The authors typically justify their choice through an asymptotic analysis using the techniques developed in Pego [57] and Cahn et al. [20], with the aim of showing that in the sharp interface limit $\varepsilon \to 0$, pure surface diffusion flux is recovered for these Cahn–Hilliard models as intended.

Interestingly, Gugenberger et al. [38], who revisited these models, pointed out an apparent inconsistency that appears in the asymptotic derivations except when the interface is flat. Their work does not show if or how the sharp interface asymptotics can be carried out correctly, and if standard surface diffusion is recovered as the limit model. However, there is some evidence that they are not merely addressing a technicality but in one case at least, when M_1 and f_p are used together, nonlinear (porous medium type) bulk diffusion is present and enters the interfacial mass flux at the same order as surface diffusion. This was oberved for example by Bray and Emmott [17] when considering the coarsening rates for dilute mixtures, and by Dai and Du [25] where the degenerate mobility holds on one, but not both sides of the interface (the work on one-sided surface diffusion by Glasner [36] and Lu et al. [52] deals with a regime where bulk diffusion from the other side is dominant and hence does not touch upon the issue). In fact, in an early publication Cahn and Taylor [19] remark that using a biquadratic potential might not drive the order parameter quickly enough towards ± 1 to sufficiently suppress bulk diffusion, citing unpublished numerical results.

In this paper, we will derive the sharp interface model for the Cahn–Hilliard equation (1.1) with the simply degenerate mobility and the quadratic polynomial for

the bulk free energy,

$$M(u) = M_1(u) \equiv \left|1 - u^2\right|, \qquad f(u) = f_p(u), \tag{1.4}$$

on a bounded two-dimensional domain Ω and show that it differs from the evolutionary equation for pure surface diffusion. Notice that this definition of the mobility allows us to also consider cases when $|u| > 1$ without incurring the type of ill-posedness that is associated with solving parabolic equations backwards in time. The equation (1.1) is supplemented with a Neumann and no-flux boundary condition,

$$\nabla_n u = M(u)\nabla_n \mu = 0, \quad \text{on } \partial\Omega. \tag{1.5}$$

The generalisation to higher dimensions is straightforward but not essential for the point we intend to make.

The matched asymptotic analysis, which is carried out for precipitates with convex interfaces, involves the matching of exponentially growing terms and multiple inner layers. It confirms that close to equilibrium, $|u| \neq 1$ in a region away from the interface layer, which in the time-dependent case allows for the possibility of significant bulk diffusion, either from one side, if $|u| \leq 1$ everywhere, or two-sided, if $u > 1$ inside the precipitate. While the existence of a solution whose values remains bounded within $[-1, 1]$ has been proven rigorously by Elliott et al. [27] for the Cahn–Hilliard equation with a degenerate mobility and initial data that lies within the same bounds, the possibility of solutions where $|u|$ takes on values larger than 1 should not be ruled out a-priori. Such solutions in fact occur in our numerical solutions if the initial data violates the bound $|u| \leq 1$ inside the precipitate.

The combination of degeneracy and a fourth order differential operator is reminiscent of thin film models [56, 24] and the sharp interface limits for the regularisation techniques used there reflect directly on the research in this paper both for sign-preserving (see e.g. [12, 13, 44, 70, 37, 26], to name just a few) and sign-changing solutions which have recently been attracting increasing attention [29, 28, 4, 15, 11, 30]. We also note that Cahn–Hilliard type equations with degenerate mobilities and various choices for the free energy, e.g. including long range forces [32], appear in other application fields such as the modelling of biofilms [46], for example, or in image processing [51], where the primary aim is not necessarily the approximation of surface diffusion.

The paper is organised as follows: Section 2 considers the asymptotic structure of the axisymmetric stationary state, which demonstrates the matched asymptotic expansion and exponential matching technique in a simpler setting. Section 3 determines the sharp interface limits to derive the free boundary problems for the interface motion, and verifies the result by comparing solutions for the sharp interface with the phase field model. Section 4 briefly considers the sharp interface limit of solutions that do not preserve the bound and for the Cahn–Hilliard model with a doubly degenerate mobility. Section 5 summarises and concludes the work.

2. Axisymmetric Stationary Solution. The aim of this paper is to investigate the sharp interface limit for the phase field model given by (1.1), (1.4), (1.5) once the solution has settled into a quasi-static state close to equilibrium and only evolves on a long time scale. We explore possible near-equilibrium states by numerically solving the model equations on an axisymmetric domain $\Omega = \{(x, y);\, r < 1\}$, where $r = (x^2 + y^2)^{1/2}$, starting with a tanh-like initial profile $u_{\text{init}}(r)$ that is bounded between -1 and 1. The result is shown in Fig. 2.1(a). The numerical solution preserves these bounds and appears to converge to a state that has a steep transition

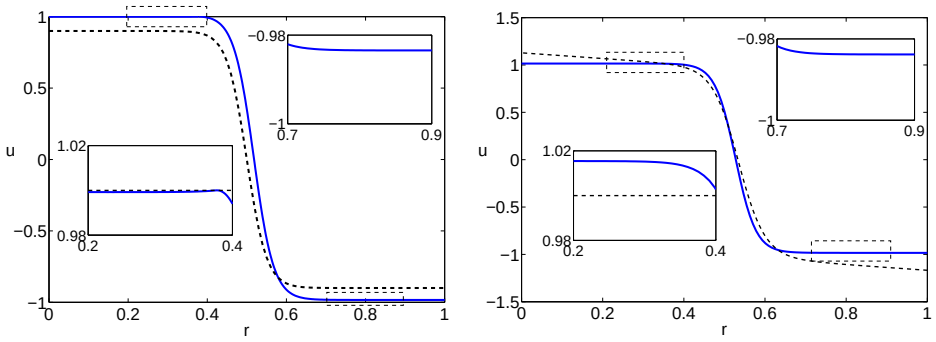

FIGURE 2.1. *The long-time solution u for the the axisymmetric degenerate Cahn–Hilliard equation* (1.1), (1.4), (1.5) *for different initial data. In (a, left panel), the initial data is bounded within* $[-1, 1]$*, while in (b, right panel) it exceeds 1 and* -1 *to the left and right, respectively. In both panels, the initial data is shown by dashed lines while the long-time solutions for* $\varepsilon = 0.05$ *at* $T = 10^4$ *are given by solid lines and have converged close to a stationary state. In (a), this stationary profile is bounded between* $[-1, 1]$*, where we emphasize that even the bump in the left inset is still below 1 (dashed line in the inset), while in (b), the upper bound 1 is exceeded for* r *less than about 0.4 (see left inset in (b)). Notice that in both (a) and (b), the value for* u *for* $r > 0.7$ *is close to but visibly larger than* -1*, by an amount that is consistent with the* $O(\varepsilon)$ *correction predicted by the asymptotic analysis (given here only for the bounds preserving case in* (2.43b)*).*

near $r_0 = 1/2$, where $u(r_0) = 0$, from a value that is very close to one for a range for $r < r_0$ and close to -1 for a range of $r > r_0$. Thus the solution approximates a single precipitate centred at the origin with an interface layer of width $O(\varepsilon)$ around r_0.

Solutions to (1.1), (1.4), (1.5) strictly monotonically decrease the total energy of the system, that is, $dE_{\rm tot}/dt < 0$ for

$$E_{\rm tot} = \int_\Omega \frac{1}{2}\varepsilon^2 |\nabla u|^2 + f_p(u). \tag{2.1}$$

Therefore, a stationary solution has to be a minimiser of $E_{\rm tot}$, subject to the boundary conditions (1.4), (1.5), a fixed volume constraint $\int_\Omega u$ =const., which arises because (1.1), (1.4), (1.5) conserve this quantity, and the constraint $|u| \le 1$. It turns out that without the last condition, the stationary solution becomes larger than 1 for a range of values $r < r_0$. This is the state that is picked out by the long-time solution of the Cahn–Hilliard equation (1.1) with a constant mobility $M = M_0$, but it can also arise for the degenerate mobility M_1. In fact, our numerical profiles for the degenerate mobility (and $f = f_p$) converged to the solution exceeding 1 for a choice of initial condition that violates the bounds $[-1, 1]$; this is shown in Fig. 2.1(b). For the bounds-preserving solution, the inequality becomes active at a point $r = r^* < r_0$. The first variation of this restricted problem therefore gives that the bounds-preserving equilibrium solution satisfies $u = 1$ for $r \le r^*$, while for $r > r^*$, we have

$$\frac{\varepsilon^2}{r}\frac{\rm d}{{\rm d}r}\left(r\frac{{\rm d}u}{{\rm d}r}\right) + \eta - 2u(u^2 - 1) = 0, \tag{2.2a}$$

with boundary conditions

$$u'(1) = 0, \tag{2.2b}$$

$$u(r^*) = 1, \qquad u'(r^*) = 0. \tag{2.2c}$$

The point r^* is a free boundary that needs to be determined as part of the problem. The constant η enters as the Lagrange parameter for the volume constraint for u. Notice that (2.2a) can be obtained directly from (1.1) by letting $u_t = 0$ and using (1.5), which also reveals that the chemical potential $\mu = \eta$. This problem needs to be supplemented by fixing the size of the precipitate either by specifying the total volume of u, or, simpler, the point r_0 where u becomes zero,

$$u(r_0) = 0. \tag{2.2d}$$

We will refer to r_0 as the location of the interface layer of the precipitate, and, borrowing from conventional use in wetting or dewetting thin film problems, to r^* and to $u'(r^*) = 0$ as the contact line and the contact angle condition, respectively. We will mostly focus on the bounds-preserving solutions and thus on this equilibrium, however, since the numerical code easily produces profiles for u that violate the inner-precipitate bound, we also record the problem statement for the corresponding equilibrium, which is given by solving (2.2) for $0 < r < 1$ and with (2.2c) replaced by

$$u'(0) = 0. \tag{2.3}$$

We will now investigate the above axisymmetric equilibrium solutions in the sharp interface limit $\varepsilon \to 0$ using matched asymptotics. This will reveal that for the specific phase field model studied here, the outer solutions, while being simple, are not trivially equal to ± 1 at all orders of magnitude, as is frequently assumed in the derivation of sharp-interface models for the Cahn–Hilliard equations [38]. This observation lies at the heart of why bulk diffusion contributes to the dynamics of the sharp interface in the fully two-dimensional (and three-dimensional) situation, which we consider in the following section. Moreover, the derivations we make here for the stationary inner problems will appear there again.

2.1. Inner layer about the interface. To elucidate the asymptotic structure of the interface, we strain the coordinates about r_0 and write

$$\rho = \frac{r - \kappa^{-1}}{\varepsilon}, \tag{2.4}$$

where we have introduced the curvature of the interface (located, as stated previously, at the zero contour line of u) via $\kappa = 1/r_0$. The resulting ODE, in the inner coordinates, reads

$$U'' + \varepsilon \frac{U'}{\kappa^{-1} + \varepsilon\rho} + \eta - 2(U^3 - U) = 0. \tag{2.5}$$

We pose the ansatz

$$U = U_0 + \varepsilon U_1 + \cdots, \tag{2.6}$$

$$\eta = \varepsilon\eta_1 + \varepsilon^2\eta_2 \cdots. \tag{2.7}$$

Here, we have used that the chemical potential $\eta \ll 1$, since in the problem (2.2) decreasing ε is equivalent to keeping ε fixed but increasing r proportionally at the same time. Thus, for $\varepsilon \to 0$, the value for η has to tend to the value for the one-dimensional equilibrium solution, which is a tanh-profile with chemical potential zero.

To leading order we have

$$U_0'' - 2(U_0^3 - U_0) = 0, \tag{2.8}$$

with the interface condition $U_0(0) = 0$. To match with the outer solution, we anticipate that U_0 need to go to a constant for $\rho \to \infty$, which can only be ± 1. By convention, we assume that u is close to one in the inside of the precipitate and close to -1 outside the precipitate, thus

$$U_0 = -\tanh \rho. \tag{2.9}$$

To $O(\varepsilon)$ we have

$$U_1'' - 2(3U_0^2 - 1)U_1 = -\eta_1 - \kappa U_0'. \tag{2.10}$$

We note that $U_0' = -\text{sech}^2\rho$ is in the kernel of the linear operator on the left-hand side of equation (2.10); thus, using the method of reduction of order and variation of parameters, the general solution is given by

$$\begin{aligned} U_1 = C_1 \text{sech}^2\rho + C_2 \text{sech}^2\rho \left(\frac{3\rho}{8} + \frac{1}{4}\sinh 2\rho + \frac{1}{32}\sinh 4\rho \right) \\ + \frac{1}{8}(2\kappa - \eta_1) + \frac{1}{48}(2\kappa - 3\eta_1)(2\cosh 2\rho - 5\,\text{sech}^2\rho). \end{aligned} \tag{2.11}$$

Requiring the interface condition $U_1(0) = 0$ and boundedness as $\rho \to \infty$ to match with the outer solution, the two constants are give by

$$C_1 = -\frac{1}{16}(\eta_1 + 2\kappa), \quad C_2 = \frac{1}{3}(3\eta_1 - 2\kappa). \tag{2.12}$$

2.2. Inner layer about the contact line. We centre the coordinates about the free boundary $\rho = \sigma$ and write

$$z = \rho + \sigma. \tag{2.13}$$

Substituting the ansatz

$$\bar{U} = 1 + \varepsilon \bar{U}_1 + \varepsilon^2 \bar{U}_2, \tag{2.14}$$

we obtain, to $O(\varepsilon)$,

$$\bar{U}_1'' - 4\bar{U}_1 = -\eta_1 \tag{2.15}$$

with initial conditions

$$\bar{U}_1(0) = \bar{U}_1'(0) = 0. \tag{2.16}$$

The solution to equation (2.15) satisfying the initial conditions (2.16) is

$$\bar{U}_1 = \frac{\eta_1}{4}\left(1 - \cosh 2z\right). \tag{2.17}$$

2.3. Exponential matching. At this stage, we have not yet made use of the condition (2.2c). We first estimate the location of the contact line in the inner coordinate $\rho = (r^* - r_0)/\varepsilon \equiv -\sigma$. Without the contact line, i.e. if we were to consider (2.2a) on the entire domain, with $u'(0) = 0$ replacing (2.2c), we would expect a solution that becomes flat for $\rho \to \infty$ and tends to a value of 1 plus a positive $O(\varepsilon)$ term. This solution intersects with $u = 1$ at $\sigma = O(\ln(1/\varepsilon))$, which is large, but tends to zero in the outer variable. Thus, (2.2c) has to be satisfied in the inner variable but since σ depends, though only logarithmically, on ε, this involves re-expanding the inner solution.

We will pursue a slightly more sophisticated approach by formulating and solving inner problems in terms of a new inner variable z centred at the contact line $\rho = -\sigma$ and then matching these solutions with the inner layer centred at the interface $\rho = 0$ using exponential matching in the spirit of Langer [49], used also in [48]. The solution centred at the interface is expanded at $\rho \to -\infty$ and the result written and re-expanded in terms of $z = \rho + \sigma$. The solution at the contact line is expanded at $z \to \infty$ and then the terms matched between the two expansions. Notice that if terms of the form $\exp(-n\rho)$, with some positive n, appear in the expansion at the interface, i.e. terms that grow for $\rho \to -\infty$, these will jump orders in ε upon rewriting them in terms of z, due to the dependence of σ on $\ln(1/\varepsilon)$.

To match expansions about the interface and the contact point free boundary, we first note that as $\rho \to -\infty$ (close to the free boundary),

$$U_0 = 1 - 2\mathrm{e}^{2\rho} + \mathrm{O}(\mathrm{e}^{4\rho}), \tag{2.18}$$

$$U_1 = \frac{1}{24}(2\kappa - 3\eta_1)\mathrm{e}^{-2\rho} + \frac{1}{2}(\kappa - \eta) + \left[\left(\frac{7\eta}{4} - \frac{11\kappa}{6}\right) + \left(\frac{3\eta}{2} - \kappa\right)\rho\right]\mathrm{e}^{2\rho} + \mathrm{O}(\mathrm{e}^{4\rho}). \tag{2.19}$$

Expressed in terms of z, Equation (2.19) reads

$$\begin{aligned} U = \Big(1 - \underbrace{2\mathrm{e}^{-2\sigma}\mathrm{e}^{2z}}_{\mathrm{A}} + O(\mathrm{e}^{4z})\Big) + \varepsilon \Bigg\{ & \underbrace{\frac{1}{24}(2\kappa - 3\eta_1)\mathrm{e}^{2\sigma}\mathrm{e}^{-2z}}_{\mathrm{B}} + \underbrace{\frac{1}{2}(\kappa - \eta_1)}_{\mathrm{C}} \\ & + \underbrace{\left[\left(\frac{7\eta_1}{4} - \frac{11\kappa}{6}\right) + \left(\frac{3\eta_1}{2} - \kappa\right)(z - \sigma)\right]\mathrm{e}^{-2\sigma}\mathrm{e}^{2z}}_{\mathrm{D}} + O(\mathrm{e}^{4z}) \Bigg\} \\ & + O(\varepsilon^2). \end{aligned} \tag{2.20}$$

The inner expansion about the free boundary can be rewritten as

$$\bar{U} = 1 + \underbrace{\frac{\varepsilon\eta_1}{4}}_{\mathrm{E}} - \underbrace{\frac{\varepsilon\eta_1}{8}\mathrm{e}^{2z}}_{\mathrm{F}} - \underbrace{\frac{\varepsilon\eta_1}{8}\mathrm{e}^{-2z}}_{\mathrm{G}} + O(\varepsilon^2). \tag{2.21}$$

The terms of the same dependence on z and ε are now matched in the expansions (2.20) and (2.21). We note that the constant terms at $O(1)$ are already matched. Matching εC and E, the constant terms at $O(\varepsilon)$, yields

$$\frac{\eta_1}{4} = \frac{1}{2}(\kappa - \eta_1) \implies \eta_1 = \frac{2}{3}\kappa. \tag{2.22}$$

Matching term A and F, we arrive at

$$2\mathrm{e}^{-2\sigma} = \frac{\varepsilon\kappa}{12}, \tag{2.23}$$

hence

$$\sigma = \frac{1}{2}\log\left(\frac{1}{\varepsilon}\right) - \frac{1}{2}\log\left(\frac{\kappa}{24}\right) + O(\varepsilon). \tag{2.24}$$

The term B does not have a counterpart in the expansion (2.21) for $\bar{U}$ and is indeed zero by virtue of (2.22). To complete matching to $O(\varepsilon)$, the terms εD and G have to be matched, which are terms of the form $\varepsilon^2\mathrm{e}^{2z}$ (after replacing σ by (2.24)) and $\varepsilon\mathrm{e}^{-2z}$. However, for this we need to include $\bar{U}_2$ and U_2 in (2.21) and (2.20), respectively, which we determine these now.

For $\bar{U}(z)$ we have

$$\bar{U}_2'' - 4\bar{U}_2 + \kappa\bar{U}_1' - 6\bar{U}_1^2 + \eta_2 = 0, \tag{2.25}$$

with initial conditions

$$\bar{U}_2(0) = \bar{U}_2'(0) = 0. \tag{2.26}$$

Substituting the equation for $\bar{U}_1$ into equation 2.25, and solving the resulting differential equation, we arrive at

$$\begin{aligned}\bar{U}_2 = &\left(\frac{\kappa}{12}\right)^2(\cosh 4z + 3\mathrm{e}^{-2z}(1+4z) - 9) + \left(\frac{\kappa}{12}\right)^2\mathrm{e}^{2z} \\ &+ \left(\frac{\kappa}{6}\right)^2\mathrm{e}^{-2z} + \frac{\eta_2}{4}(1-\cosh 2z).\end{aligned} \tag{2.27}$$

The $O(\varepsilon^2)$ ODE for $U(\rho)$ is given by

$$\begin{aligned}U_2'' - 2(3U_0^2-1)U_2 &= -\eta_2 - \kappa U_1' + \rho\kappa^2 U_0' + 6U_0U_1^2 \\ &= -\eta_2 - \frac{\kappa^2}{6}\tanh^5\rho - \rho\kappa^2\mathrm{sech}^2\rho - \frac{\kappa^2}{3}\tanh\rho\,\mathrm{sech}^2\rho.\end{aligned} \tag{2.28}$$

As in the solution of Equation (2.10), the general solution is given by

$$U_2 = P(\rho) + C_1\mathrm{sech}^2\rho + C_2\mathrm{sech}^2\rho\left(\frac{3\rho}{8} + \frac{1}{4}\sinh 2\rho + \frac{1}{32}\sinh 4\rho\right), \tag{2.29}$$

where

$$\begin{aligned}P(\rho) = &-\frac{\eta_2}{8} - \frac{\rho\kappa^2}{4} - \frac{1}{8}\cosh 2\rho\left(\eta_2 + \frac{2}{3}\rho\kappa^2\right) + \frac{1}{16}\mathrm{sech}^2\rho\left(5\eta_2 + \frac{23}{6}\rho\kappa^2 - 2\rho^2\kappa^2\right) \\ &+ \frac{1}{4}\rho\kappa^2\log\left(\frac{1}{2}\mathrm{e}^{\rho}\right)\mathrm{sech}^2\rho + \frac{\kappa^2}{8}\mathrm{sech}^2\rho\,\mathrm{Li}_2(-\mathrm{e}^{2\rho}) \\ &- \frac{\kappa^2}{288}\sinh 2\rho\,(1 - 24\log\cosh\rho) \\ &- \frac{\kappa^2}{96}\tanh\rho\left(1 - 24\log\cosh\rho - \frac{8}{3}\mathrm{sech}^2\rho\right),\end{aligned} \tag{2.30}$$

and $\mathrm{Li}_2(x)$ is the dilogarithm function. Boundedness as $\rho \to \infty$ to enable matching to the outer solution, and the interface condition $U_2(0) = 0$ allow the determination of the two constants in terms of η_2:

$$C_1 = \frac{1}{16}\left(\frac{\pi^2}{6}\kappa^2 - \eta_2\right), \quad C_2 = \frac{\kappa^2}{36}(1 + 24\log 2) + \eta_2. \tag{2.31}$$

To match the asymptotic expansions for the two interior layers, it turns out that we also need to include corrections for σ, thus we expand the position of the free boundary as an ascending power series of ε, *viz.*

$$\sigma = \sigma_0 + \varepsilon\sigma_1 + \cdots, \tag{2.32}$$

with the leading order term, σ_0, already given by equation (2.24). Including higher order exponential terms in the expansion of U_0 and U_1 as $\rho \to -\infty$, we have

$$U_0 = 1 - \frac{\varepsilon\kappa}{12}\mathrm{e}^{2\mathrm{z}}(1 - 2\varepsilon\sigma_1) + \frac{1}{2}\left(\frac{\varepsilon\kappa}{12}\right)^2 \mathrm{e}^{4\mathrm{z}} + \mathrm{O}(\varepsilon^3), \tag{2.33}$$

$$U_1 = \frac{\kappa}{6} - \frac{\varepsilon\kappa^2}{36}\mathrm{e}^{2\mathrm{z}} + \mathrm{O}(\varepsilon^2), \tag{2.34}$$

$$U_2 = -\frac{1}{8}\eta_2\left(\frac{24}{\varepsilon\kappa}\right)(1 + 2\varepsilon\sigma_1)\mathrm{e}^{-2\mathrm{z}} + \left(\frac{\eta_2}{4} - \frac{\kappa^2}{16}\right) + \mathrm{O}(\varepsilon). \tag{2.35}$$

Thus, by combining U_0, U_1 and U_2,

$$\begin{aligned} U = 1 &- \frac{\varepsilon\kappa}{12}\mathrm{e}^{2\mathrm{z}}(1 - 2\varepsilon\sigma_1) + \frac{1}{2}\left(\frac{\varepsilon\kappa}{12}\right)^2 \mathrm{e}^{4\mathrm{z}} + \varepsilon\left(\frac{\kappa}{6} - \frac{\varepsilon\kappa^2}{36}\mathrm{e}^{2\mathrm{z}}\right) \\ &+\varepsilon^2\left[-\frac{1}{8}\eta_2\left(\frac{24}{\varepsilon\kappa}\right)(1 + 2\varepsilon\sigma_1)\mathrm{e}^{-2\mathrm{z}} + \left(\frac{\eta_2}{4} - \frac{\kappa^2}{16}\right)\right] + O(\varepsilon^3). \end{aligned} \tag{2.36}$$

Writing out the expansion for $\bar{U}$, we have

$$\begin{aligned} \bar{U} = 1 &+ \varepsilon\frac{\kappa}{6}(1 - \cosh 2z) \\ &+ \varepsilon^2\left[\frac{1}{2}\left(\frac{\kappa}{12}\right)^2 \mathrm{e}^{4\mathrm{z}} + \frac{1}{2}\left(\frac{\kappa}{12}\right)^2 \mathrm{e}^{-4\mathrm{z}} + \left(\frac{\kappa}{12}\right)^2 (3\mathrm{e}^{-2\mathrm{z}}(1 + 4\mathrm{z}) - 9)\right. \\ &\left. + \left(\frac{\kappa}{12}\right)^2 \mathrm{e}^{2\mathrm{z}} + \left(\frac{\kappa}{6}\right)^2 \mathrm{e}^{-2\mathrm{z}} + \frac{\eta_2}{4}(1 - \cosh 2\mathrm{z})\right]. \end{aligned} \tag{2.37}$$

We first match the decaying exponential $\mathrm{e}^{-2\mathrm{z}}$ at $O(\varepsilon)$ in equation (2.37) to its counterpart in U_2, arriving at

$$\frac{1}{8}\frac{24}{\kappa}\eta_2 = \frac{\kappa}{12} \implies \eta_2 = \left(\frac{\kappa}{6}\right)^2. \tag{2.38}$$

To obtain σ_1, it is most convenient to match the coefficient of the growing term $\mathrm{e}^{2\mathrm{z}}$ at $O(\varepsilon^2)$. Matching them, we arrive at

$$\left(\frac{\kappa}{12}\right)^2 - \frac{1}{8}\eta_2 = \frac{\kappa}{6}\sigma_1 - \left(\frac{\kappa}{6}\right)^2 \implies \sigma_1 = \frac{3\kappa}{16}. \tag{2.39}$$

Thus

$$\sigma = \frac{1}{2}\log\left(\frac{1}{\varepsilon}\right) - \frac{1}{2}\log\left(\frac{\kappa}{24}\right) + \frac{3\kappa}{16}\varepsilon + O(\varepsilon^2), \tag{2.40}$$

$$\eta = \frac{2\kappa}{3}\varepsilon + \frac{\kappa^2}{36}\varepsilon^2 + O(\varepsilon^3). \tag{2.41}$$

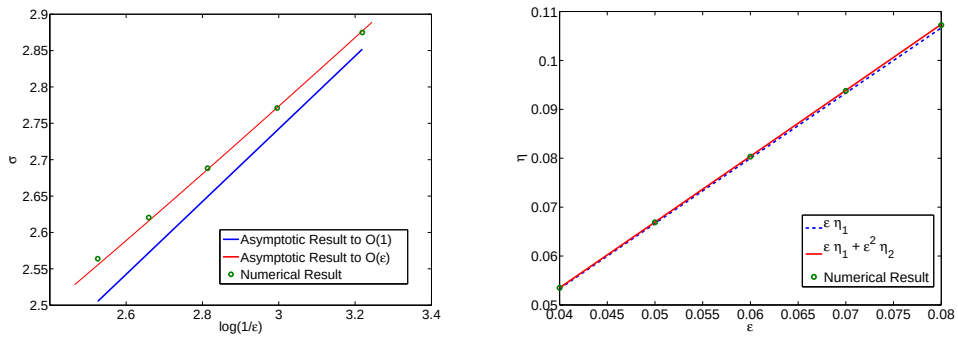

FIGURE 2.2. *Comparing the asymptotic and numerical results for (left) the position of the free boundary and (right) the chemical potential, for a range of ε and fixed $r_0 = 1/2$. The position of the free boundary is obtained via solving the ODE free boundary problem (2.2) using Matlab package ode15s to 10^{-10} accuracy, and placing the interface at $r_0 = 0.5$ to 10^{-10} accuracy via adjusting the excess potential η using the method of bisection.*

Figure 2.2 shows that the asymptotic expansion agrees well with the position of the free boundary and the chemical potential obtained via numerical solution of the ODE free boundary problem (2.2), confirming the validity of the matched asymptotic expansions.

2.4. Outer solutions. While the bound-preserving equilibrium state is equal to 1 at $r = r_0 - \varepsilon\sigma$ and below, outside the precipitate, u remains bounded from -1 and therefore the outer expansion on the exterior of the precipitate is *not* equal to -1 to all orders of ε. The non-trivial corrections must be consistently determined by solving the outer problems order by order and then checked that they match with the inner layer at the interface using standard matching principles [39, 43]. We stress that this is a key difference with some of the literature, which resolves the inconsistency in the asymptotic analysis observed by Gugenberger et al. [38], and leads to nonlinear bulk diffusion in the sharp interface limit in the time-dependent version of phase field model. Inserting the ansatz

$$u = u_0 + \varepsilon u_1 + \varepsilon u_2 \cdots \tag{2.42}$$

into equation (2.2a), we arrive at the following outer problems and solutions,

$$O(1): \quad u_0(u_0^2 - 1) = 0 \qquad \Longrightarrow \quad u_0 = -1, \tag{2.43a}$$

$$O(\varepsilon): \quad 2(3u_0^2 - 1)u_1 = \eta_1 \qquad \Longrightarrow \quad u_1 = \frac{\kappa}{6} \tag{2.43b}$$

$$O(\varepsilon^2): \quad 2(3u_0^2 - 1)u_2 = \eta_2 - 6u_0u_1 \qquad \Longrightarrow \quad u_2 = \frac{7}{4}\left(\frac{\kappa}{6}\right)^2, \tag{2.43c}$$

where we have used the results for the expansion of $\mu = \eta$, which are constants for the equilibrium state. The outer solutions are thus also constants, all of which match the inner solutions, i.e., $u_i = \lim_{\rho\to\infty} U_i(\rho)$ for $i = 0, 1, 2$, as can be verified by calculating the limits from (2.8), (2.11) and (2.29).

3. Sharp Interface Dynamics.

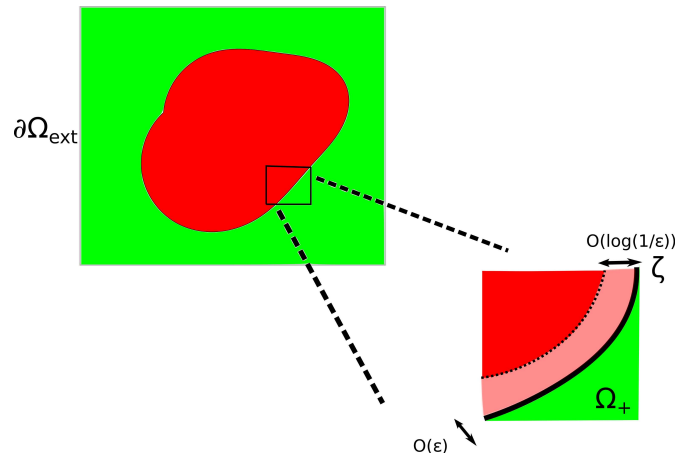

FIGURE 3.1. *Illustration of the asymptotic structure of the degenerate mobility case. The dotted line indicates the contact line free boundary beyond which $u = 1$, and the solid line denotes the interface. There are interior layers about the contact line and interface respectively, and an outer layer outside the precipitate (the green region Ω_+).*

3.1. Outer variables. Motivated by the stationary state, we consider the asymptotic structure of the dynamical problem for a deformed precipitate, comprising of an outer layer away from the interface, an interior layer about the interface, and, further to the inside of the preicipitate, a region where u is below and arbitrarily close to 1. In fact, it is useful to consider the limit where $1 - u \searrow 0$. This approach is similar in spirit to the "precursor" regularisation used in thin film problems, see for example [44], where the free boundary problem that arises in the limit of vanishingly small precursor thickness was determined by matched asymptotics. The corresponding analysis for the situation is carried out in the appendix, and it shows that to leading order, we obtain a free boundary problem consisting of equations (1.1), (1.4), (1.5) and a contact line $\Gamma(t)$ as the free boundary, with conditions

$$u = 1, \qquad \mathbf{n}_\Gamma \cdot \nabla u = 0, \qquad \mathbf{n}_\Gamma \cdot \mathbf{j} = 0 \qquad \text{at } \Gamma, \tag{3.1a}$$

as determined from the matched asymptotic analysis. Here, $\mathbf{n}_\Gamma$ denotes the normal to the curve given by Γ. In the context of wetting or dewetting liquid films, the second condition has the meaning of a zero contact angle condition.

For the subsequent analysis, we need to choose an appropriate time scale. Consider a circular precipitate at equilibrium where the interface, i.e. the zero contour of the order parameter is subject to corrugations over an $O(1)$ length scale. This will thus also deform μ over these length scales. Since near equilibrium μ and $1 - u$, and therefore also $M(u) = 1 - u^2$, are $O(\varepsilon)$, it follows that $\mathbf{j} = O(\varepsilon^2)$, thus $u_t = O(\varepsilon^2)$. Therefore, the evolution of the order parameter occurs over an $O(1/\varepsilon^2)$ time scale. We have estimated here the expected contribution from diffusion away from the interface, i.e. bulk diffusion, but this is also the time scale chosen in the literature to capture the contribution from surface diffusion, see [20]. Thus we already have an indication that both effects will determine the interface evolution to the same order.

In any case, we rescale time via $\tau = \varepsilon^2 t$, so that the Cahn–Hilliard equation reads

$$\varepsilon^2 \partial_\tau u = \nabla \cdot \mathbf{j}, \qquad \mathbf{j} = M(u)\nabla\mu, \qquad \mu = -\varepsilon^2 \nabla^2 u + f'(u), \tag{3.1b}$$

with mobility and free energy $M = M_1$, $f = f_p$, see (1.4), and boundary conditions

$$\nabla_n u = 0, \qquad M(u)\nabla_n \mu = 0 \qquad \text{on } \partial\Omega. \tag{3.1c}$$

For the outer expansions, we will use

$$\begin{aligned} u &= u_0 + \varepsilon u_1 + \varepsilon^2 u_2 \cdots, \\ \mu &= \mu_0 + \varepsilon \mu_1 + \varepsilon^2 \mu_2 \cdots, \\ \mathbf{j} &= \mathbf{j}_0 + \varepsilon \mathbf{j}_1 + \varepsilon^2 \mathbf{j}_2 \cdots. \end{aligned}$$

3.2. Inner variables. As in [57, 38], we define the local coordinates relative to the position of the interface (parametrised by s), and write

$$\mathbf{r}(s, r, \tau) = \mathbf{R}(s, \tau) + r\mathbf{n}(s, \tau), \tag{3.2}$$

where $\mathbf{R}$, the position of the interface ζ, is defined by

$$u(\mathbf{R}, t) = 0, \tag{3.3}$$

and $\mathbf{t} = \partial\mathbf{R}/\partial s$ is the unit tangent vector, and $\mathbf{n}$ is the unit outward normal. From the Serret-Frenet formulae in 2D we have that $\kappa\mathbf{t} = \partial\mathbf{n}/\partial s$, thus

$$\frac{\partial \mathbf{r}}{\partial r} = \mathbf{n}(s), \qquad \frac{\partial \mathbf{r}}{\partial s} = (1 + r\kappa)\mathbf{t}(s), \tag{3.4}$$

where $\mathbf{t}(s)$ is the unit tangent vector to the interface, and κ is the curvature. We adopt the convention that the curvature is positively defined if the osculating circle lies inside the precipitate, which we will define to be the "+" phase. The gradient operator in these curvilinear coordinates reads

$$\nabla = \mathbf{n}\partial_r + \frac{1}{1 + r\kappa}\mathbf{t}\,\partial_s, \tag{3.5}$$

and the divergence operator of a vector field $\mathbf{A} \equiv A_r\mathbf{n} + A_s\mathbf{t}$ reads

$$\nabla \cdot \mathbf{A} = \frac{1}{1 + r\kappa}\left[\partial_r\Big((1 + r\kappa)A_n\Big) + \partial_s\left(\frac{1}{1 + r\kappa}A_s\right)\right]. \tag{3.6}$$

We let s and $\rho = r/\varepsilon$ be the inner coordinates at the interface, and let $U(\rho, s, \tau)$, $\eta(\rho, s, \tau)$ and $\mathbf{J}(\rho, s, \tau)$ denote the order parameter, chemical potential and flux written in these coordinates, respectively. We will expand these as

$$\begin{aligned} U &= U_0 + \varepsilon U_1 + \varepsilon^2 U_2 \cdots, \\ \eta &= \eta_0 + \varepsilon \eta_1 + \varepsilon^2 \eta_2 \cdots, \\ \mathbf{J} &= \varepsilon^{-1}\mathbf{J}_{-1} + \mathbf{J}_0 + \varepsilon \mathbf{J}_1 + \varepsilon^2 \mathbf{J}_2 \cdots. \end{aligned}$$

In inner coordinates about the interface, the first two equations in (3.1b) combined become

$$\varepsilon^2 \partial_\tau U - \varepsilon v_n \partial_\rho U = \nabla \cdot (M(U)\nabla\eta), \tag{3.7a}$$

with $v_n = \mathbf{R}_\tau \cdot \mathbf{n}$ and where, using equations (3.5) and (3.6),

$$\begin{aligned}\nabla \cdot (M(U)\nabla) = \varepsilon^{-2}&\partial_\rho M(U_0)\partial_\rho \\ &+\varepsilon^{-1}\Big\{\partial_\rho\Big(\kappa\rho M(U_0) + M'(U_0)U_1\Big)\partial_\rho - \kappa\rho\,\partial_\rho M(U_0)\partial_\rho\Big\} \\ &+\Big\{\kappa^2\rho^2\partial_\rho M(U_0)\partial_\rho - \kappa\rho\partial_\rho\Big(\kappa\rho M(U_0) + M'(U_0)U_1\Big)\partial_\rho \\ &+\partial_\rho\Big(\kappa\rho M'(U_0)U_1 + \frac{1}{2}M''(U_0)U_1^2 + M'(U_0)U_2\Big)\partial_\rho \\ &+\partial_s M(U_0)\partial_s\Big\} + O(\varepsilon). \qquad (3.7b)\end{aligned}$$

Taking only the first equation in (3.1b) we have

$$\varepsilon^2\partial_\tau U - \varepsilon v_n\partial_\rho U = \frac{1}{1+\varepsilon\rho\kappa}\left[\varepsilon^{-1}\partial_\rho\Big((1+\varepsilon\rho\kappa)J_n\Big) + \partial_s\left(\frac{1}{1+\varepsilon\rho\kappa}J_s\right)\right]. \qquad (3.8)$$

In inner coordinates, we will only need to know the normal component $J_n = \mathbf{n}\cdot\mathbf{J}$ of the flux explicitly in terms of the order parameter and chemical potential. It is given by

$$\begin{aligned}J_n &= \frac{M(U)}{\varepsilon}\partial_\rho\eta \\ &= \varepsilon^{-1}M(U_0)\partial_\rho\eta_0 + M'(U_0)U_1\partial_\rho\eta_0 + M(U_0)\partial_\rho\eta_1 \\ &\quad + \varepsilon\left(M(U_0)\partial_\rho\eta_2 + M'(U_0)U_1\partial_\rho\eta_1 + M'(U_0)U_2\partial_\rho\eta_0 + \frac{1}{2}M''(U_0)U_1^2\partial_\rho\eta_0\right) \\ &\quad + \varepsilon^2\left[M(U_0)\partial_\rho\eta_3 + M'(U_0)U_1\partial_\rho\eta_2 + \left(M'(U_0)U_2 + \frac{1}{2}M''(U_0)U_1^2\right)\partial_\rho\eta_1\right. \\ &\qquad \left. + \left(M'(U_0)U_3 + M''(U_0)U_1U_2 + \frac{1}{6}M'''(U_0)U_1^3\right)\partial_\rho\eta_0\right] + O(\varepsilon^3), \qquad (3.9)\end{aligned}$$

which also motivates our ansatz for the expansion for $\mathbf{J}$.

Moreover, s and $z = \rho + \sigma(s,t)$ are the coordinates for the inner layer about the contact line, and the order parameter, chemical potential and flux in these variables are given by $\bar{U}(z,s,\tau)$, $\bar{\eta}(z,s,\tau)$ and $\bar{\mathbf{J}}(z,s,\tau)$, respectively, with expansions

$$\begin{aligned}\bar{U} &= \bar{U}_0 + \varepsilon\bar{U}_1 + \varepsilon^2\bar{U}_2\cdots, \\ \bar{\eta} &= \bar{\eta}_0 + \varepsilon\bar{\eta}_1 + \bar{\varepsilon}^2\bar{\eta}_2\cdots, \\ \bar{\mathbf{J}} &= \varepsilon^{-1}\bar{\mathbf{J}}_{-1} + \bar{\mathbf{J}}_0 + \varepsilon\bar{\mathbf{J}}_1 + \varepsilon^2\bar{\mathbf{J}}_2\cdots.\end{aligned}$$

Thus, the equations for the inner coordinates about the contact line are found by applying the substitution $\rho = z + \sigma(s,\tau)$ and using the "bar" notation for the dependent variables.

Notice that the location where the two inner layers are centred depends on ε and therefore, in principle, σ and also R need to be expanded in terms of ε as well. However, we are only interested in the leading order interface motion, so to keep the notation simple, we use σ and R and their leading order contributions interchangeably. We now solve and match the outer and inner problems order by order.

3.3. Matching.

Leading order. For the outer problem, we obtain to leading order

$$\begin{aligned} \nabla \cdot \mathbf{j}_0 &= 0, \\ \mathbf{j}_0 &= M(u_0)\nabla \mu_0, \\ \mu_0 &= f'(u_0). \end{aligned} \tag{3.10}$$

The requisite boundary conditions are $\nabla_n u = 0$, and $\mathbf{n} \cdot \mathbf{j}_0 = 0$ on $\partial\Omega_{\text{ext}}$. Following our convention that the "$-$" phase is outside the precipitate, we have

$$u_0 = -1, \qquad \mu_0 = 0. \tag{3.11}$$

The leading order expansion about the interface reads

$$\partial_\rho \left(M(U_0)\partial_\rho \eta_0 \right) = 0, \tag{3.12a}$$

$$f'(U_0) - \partial_{\rho\rho} U_0 = \eta_0. \tag{3.12b}$$

Integrating once in ρ, we obtain

$$M(U_0)\partial_\rho \eta_0 = a_1(s,\tau). \tag{3.13}$$

From the matching condition, we require

$$\lim_{\rho\to\infty} U_0(\rho) = -1. \tag{3.14}$$

Taking this limit in (3.12b) gives $\eta_0 \to 0$ and this implies $a_1 = 0$, therefore also $\eta_0 = 0$, which matches with μ_0. Moreover, from (3.12a) and (3.14), we have

$$U_0 = -\tanh \rho. \tag{3.15}$$

Using the result for η_0 and (3.9), we also conclude that $J_{n,-1} = 0$.

The leading order approximation of the order parameter about the contact line is easily found to be $\bar{\mathbf{U}}_0 = 1$, and also for the chemical potential $\bar{\eta}_0 = 0$, and the normal component of the flux $\bar{J}_{n,-1} = 0$.

O(ε) correction. The first two parts of the outer correction problem for (3.1b) are automatically satisfied, since $\mu_0 = 0$ and $M(u_0) = 0$, by

$$\mathbf{j}_1 = 0. \tag{3.16}$$

The last part requires

$$\mu_1 = f''(u_0)u_1 = 4u_1. \tag{3.17}$$

From (3.7), and noting that $\eta_0 = 0$, we have

$$\partial_\rho \left(M(U_0)\partial_\rho \eta_1 \right) = 0, \tag{3.18}$$

thus $M(U_0)\partial_\rho \eta_1 = \eta_1(s,\tau)$ is constant in ρ. However, from (3.9), we see that this expression is simply the normal flux term $J_{n,0}$, which has to match with j_0 hence is zero. Therefore, η does not depend on ρ. Now, equation (3.18) is the same as equation (2.10) in the previous section on the axisymmetric stationary state. As

such, the general solution that satisfies the interfacial condition $U_1(0, s, \tau) = 0$ and $U_1(\rho, s, \tau)$ bounded as $\rho \to \infty$ is given by equation (2.11).

The $O(\varepsilon)$ problem about the contact line free boundary becomes

$$\bar{\eta}_1 = -\partial_{zz}\bar{U}_1 + 4\bar{U}_1, \tag{3.19}$$

with $\bar{\eta}_1$ that does not depend on z, supplemented with the conditions $\bar{U}_1(z, 0, \tau) = 1$, $\bar{U}_{1z}(z, 0, \tau) = 0$. This equation is the same as the $O(\varepsilon)$ equation for the stationary state about the free boundary, and the solution is given by (2.17).

The inner layers about the contact line and about the interface can be exponentially matched, as outlined in section 2.3, to obtain

$$\eta_1 = \frac{2}{3}\kappa. \tag{3.20}$$

$O(\varepsilon^2)$ correction. Combining the first two equations in (3.1b) and expanding to $O(\varepsilon^2)$ yields

$$\nabla \cdot (M'(u_0)u_1 \nabla \mu_1) = 0. \tag{3.21}$$

Equation (3.17) provides a relation between μ_1 and u_1. Noting that for mobility $M = M_1$, the coefficient $M'(u_0)$ is a constant, we have

$$\nabla \cdot (\mu_1 \nabla \mu_1) = 0. \tag{3.22}$$

The boundary conditions are $\nabla_n \mu_1 = 0$ on $\partial\Omega_{\text{ext}}$, and, from matching μ_1 with η_1 (given in (3.20)) at the interface,

$$\mu_1 = \frac{2}{3}\kappa. \tag{3.23}$$

Expanding the second equation in (3.1b) to $O(\varepsilon^2)$ also gives us an expression for the normal flux

$$\mathbf{n} \cdot \mathbf{j}_2 = u_1 M'(u_0) \nabla_n \mu_1 = \frac{1}{2}\mu_1 \nabla_n \mu_1, \tag{3.24}$$

which is not in general zero.

Inner expansion about the interface. From the $O(1)$ terms in (3.7), we obtain

$$\partial_\rho \left(M(U_0) \partial_\rho \eta_2 \right) = 0. \tag{3.25}$$

Thus, $M(U_0)\partial_\rho \eta_2$ is constant in ρ and since we can identify this expression via (3.9) as $J_{n,1}$, which has to match with $\mathbf{n} \cdot \mathbf{j}_1 = 0$, we can deduce that

$$J_{n,1} = M(U_0)\partial_\rho \eta_2 = 0. \tag{3.26}$$

Therefore, η_2 is independent of ρ. The solution for η_2 is found in essentially the same way as in section 2, equations (2.25)-(2.38), thus

$$\eta_2(s, \tau) = \frac{\kappa^2}{36}. \tag{3.27}$$

$\mathbf{O}(\varepsilon^3)$ correction. Noting that η_0, η_1 and η_2 are independent of ρ, the $O(\varepsilon)$ terms in (3.7) yield

$$\begin{aligned} -v_n\partial_\rho U_0 &= \partial_\rho M(U_0)\partial_\rho\eta_3 + \partial_s M(U_0)\partial_s\eta_1 \\ &= \partial_\rho M(U_0)\partial_\rho\eta_3 + \frac{2}{3}M(U_0)\partial_{ss}\kappa. \end{aligned} \tag{3.28}$$

Integrating equation (3.28) from $-\infty$ to ∞, we arrive at

$$v_n = \frac{1}{2}[M(U_0)\partial_\rho\eta_3]_{-\infty}^{\infty} + \frac{2}{3}\partial_{ss}\kappa. \tag{3.29}$$

From (3.9), we can identify the term in the brackets as

$$J_{n,2} = M(U_0)\partial_\rho\eta_3. \tag{3.30}$$

At $\rho \to -\infty$, we need to match this (via exponential matching) with the solution for $\bar{\eta}_3$ and $\mathbf{n}\cdot\bar{\mathbf{J}}_2$ at the contact line, which in the latter case is just zero, and in the former is a function independent of z. Thus, η_3 is matched to a constant for $\rho \to \infty$, and $J_{n,2}$ is matched to zero, thus

$$\lim_{\rho\to-\infty} J_{n,2} = \lim_{\rho\to-\infty} M(U_0)\partial_\rho\eta_3 = 0. \tag{3.31}$$

We next consider the contribution from the term at $\rho \to \infty$. It is tempting to argue that, since $M(U_0) \to 0$ exponentially fast, this term has to be zero. However, this would imply, from (3.30), that $J_{n,2} = 0$, which cannot be matched with $\mathbf{n}\cdot\mathbf{j}_2$. Instead, we match the normal fluxes,

$$\lim_{\rho\to\infty} J_{n,2} = \mathbf{n}\cdot\mathbf{j}_2|_\zeta\,,$$

where ζ denotes the interface. Thus

$$\lim_{\rho\to\infty} M(U_0)\partial_\rho\eta_3 = \frac{1}{2}\mu_1\nabla_n\mu_1|_\zeta. \tag{3.32}$$

However, we now have to accept exponential growth in η_3 at $\rho \to \infty$. In fact, solving for η_3 explicitly using (3.29), (3.31), (3.32), we obtain

$$\eta_3 = \frac{\mu_1\nabla_n\mu_1|_\zeta}{8M'(-1)}\mathrm{e}^{2\rho} + \frac{\rho}{2\mathrm{M}'(-1)} + \eta_3^0, \tag{3.33}$$

where η_3^0 is an integration constant. The $\mathrm{e}^{2\rho}$ term does not seem to be matchable to the outer solution. We will resolve this issue in a separate section, by introducing another inner layer, and for now use the expression (3.32) in (3.29).

All in all, the sharp interface problem is given by

$$\nabla\cdot(\mu_1\nabla\mu_1) = 0, \quad \text{in } \Omega_+, \tag{3.34a}$$

$$\mu_1 = \frac{2}{3}\kappa, \quad \text{on } \zeta, \tag{3.34b}$$

$$\nabla_n\mu_1 = 0, \quad \text{on } \partial\Omega_{\text{ext}}, \tag{3.34c}$$

$$v_n = \frac{2}{3}\partial_{ss}\kappa + \frac{1}{4}\mu_1\nabla_n\mu_1 \quad \text{on } \zeta. \tag{3.34d}$$

Besides the usual surface diffusion term, equation (3.34) contains an additional normal flux term which is nonlocal, i.e. couples the interface motion with nonlinear bulk diffusion. The implications of this contribution are particularly dramatic in a situation with multiple unconnected precipitates, the normal mass flux enables larger precipitates to grow at the expense of smaller precipitates similar to the coarsening behaviour for the Cahn–Hilliard equation with constant mobility, but is not expected for pure surface diffusion. However, even for a single precipitate that is slightly perturbed from its axisymmetric state, the effect on the relaxation dynamics is noticeable, as we now explore.

3.4. Linear stability analysis. To compare the sharp interface model with the phase field model, we consider the relaxation of an azimuthal perturbation to an axisymmetric stationary state with curvature $\kappa = 1/r_0$. For azimuthal perturbations proportional to $\cos m\theta$, the pure solid diffusion model $v_n = \mathfrak{M}\partial_{ss}\kappa$ predicts an exponential decay rate

$$\sigma = -\mathfrak{M}\frac{m^2(m^2-1)}{r_0^4}. \tag{3.35}$$

In contrast, the decay rate in the porous medium model, equation (3.34), is given by

$$\sigma = -\frac{2}{3}\frac{m^2(m^2-1)}{r_0^4} - \frac{1}{9}\frac{m(m^2-1)}{r_0^4}\tanh(m\log r_0^{-1}). \tag{3.36}$$

In the diffuse interface model, the perturbation $v_1(r,t)\cos m\theta$ satisfies

$$\begin{aligned} v_{1t} &= \frac{1}{r}\frac{\partial}{\partial r}\left(rM(v_0)\frac{\partial \mathfrak{m}_1}{\partial r}\right) - \frac{m^2}{r^2}M(v_0)\mathfrak{m}_1, \\ \mathfrak{m}_1 &= -\frac{\varepsilon^2}{r}\frac{\partial}{\partial r}\left(r\frac{\partial v_1}{\partial r}\right) + \left(\frac{m\varepsilon}{r}\right)^2 v_1 + f''(v_0)v_1, \end{aligned} \tag{3.37}$$

where $v_0(r)$ is the axisymmetric stationary state. We solve this system numerically, using the Chebyshev spectral collocation method (see Appendix) with $\Delta t = 10^{-3}$ and 400 mesh points until $T = 1/\varepsilon^2$. The decay rate of the eigenfunction is tracked by monitoring its maximum. The diffuse interface decay rates are scaled with $1/\varepsilon^2$ to compare with the sharp interface model. The base state that is needed for this calculation is determined a-priori with the interface, i.e. the zero contour, positioned at $r_0 = 0.5$.

The initial condition for the perturbation,

$$v_1(0,r) = \exp\left(\frac{1}{a^2-(r_0-r)^2}\right), \tag{3.38}$$

acts approximately as a shift to the leading order shape of the inner layer. The constant a is chosen so that the support of $v_1(0,r)$ lies within the inner layer, to avoid introducing a perturbation beyond the contact line of the base state (i.e. for $r < r_*$).

The results are compared in Table 3.1. They show that the decay rate of the azimuthal perturbation to the axisymmetric base state obtained for $m = 2$ tends to the eigenvalue for the linearised sharp interface model *with* the contribution from nonlinear bulk diffusion, rather than to the one for pure surface diffusion. This confirms that (3.34) describes the leading oder sharp interface evolution for the Cahn–Hilliard model with mobility $M = M_1$ and $f = f_p$ correctly, and that the sharp interface motion is distinct from the one induced by pure surface diffusion.

ε	0.01	0.005	0.003	0.002	0.001	**Eq (3.36)**	**Eq (3.35)**
$\sigma_{m=2}$	-133.2	-133.8	-136.0	-136.3	-137.0	$\mathbf{-137.4}$	$\mathbf{-128}$

TABLE 3.1

Relaxation rates obtained from the linearised phase field model (3.37) are shown for different values of ε in the first five columns, and compared to the eigenvalues obtained for linearised sharp interface models for pure surface diffusion (3.35) *and the porous medium type model* (3.36) *in the next-to-last and the last column, respectively, with $\mathfrak{M} = 2/3$.*

3.5. Closing the matching for the chemical potential. The exponential growth of η_3 at $\rho \to \infty$ is a direct consequence of the exponential decay of $M(U_0)$ to 0 as U_0 approaches -1 exponentially fast. Notice, however, that the inner solution including the correction terms does not decay to -1, because $U_1(\rho \to \infty) > 0$, so that

$$M(U_0 + \varepsilon U_1 + \cdots) = M(U_0) + \varepsilon M'(U_0)U_1 + \cdots$$

approaches a non-zero $O(\varepsilon)$ value as $\rho \to \infty$. We need to ensure that the correction $\varepsilon M'(U_0)U_1$ to $M(U_0)$ enters into the calculation of the chemical potential as soon as ρ is in the range where $M(U_0)$ and $\varepsilon M'(U_0)U_1$ have the same order of magnitude. This happens when $U_0 + 1 = O(\varepsilon)$, i.e. when $\rho \sim -(1/2)\ln\varepsilon$. We therefore introduce another layer via

$$\rho = \frac{1}{2}\ln\left(\frac{1}{\varepsilon}\right) + y,$$
$$\hat{U}(y) = U(\rho), \qquad \hat{\eta}(y) = \eta(\rho), \qquad \hat{\mathbf{J}}(y) = \mathbf{J}(\rho).$$

Notice the similarity with the expansion at the contact line. Indeed, the solution in the new layer will have exponential terms in the expansion at $y \to -\infty$ that need to be matched with the terms in the expansion of the solution at the interface for $y \to \infty$.

In terms of the new variables, the Cahn–Hilliard equation becomes

$$\varepsilon^2\partial_\tau\hat{U} - \varepsilon v_n\partial_y\hat{U} = \nabla\cdot\left(M(\hat{U})\nabla\hat{\eta}\right), \tag{3.39}$$

$$\hat{\eta} = -\partial_{yy}\hat{U} - \frac{\varepsilon\kappa}{1+\varepsilon\kappa\left(y-\frac{1}{2}\ln\varepsilon\right)}\partial_y\hat{U} - \frac{\varepsilon^2}{1+\varepsilon\kappa\left(y-\frac{1}{2}\ln\varepsilon\right)}\partial_s\left(\frac{\partial_s\hat{U}}{1+\varepsilon\kappa\left(y-\frac{1}{2}\ln\varepsilon\right)}\right) + f'(\hat{U}). \tag{3.40}$$

We expand

$$\hat{U} = -1 + \varepsilon\hat{U}_1 + \varepsilon^2\hat{U}_2 + \cdots, \tag{3.41a}$$
$$\hat{\eta} = \varepsilon\hat{\eta}_1 + \hat{\varepsilon}^2\hat{\eta}_2 + \cdots,$$
$$\hat{\mathbf{J}} = \hat{\mathbf{J}}_0 + \varepsilon\hat{\mathbf{J}}_1 + \varepsilon^2\hat{\mathbf{J}}_2 + \cdots, \tag{3.41b}$$

which gives

$$\nabla\cdot\left(M(\hat{U})\nabla\hat{\eta}\right) = \partial_y\left[M'(-1)\hat{U}_1\partial_y\hat{\eta}_1\right] + \varepsilon\partial_y\left[M'(-1)\hat{U}_1\partial_y\hat{\eta}_2\right] + O(\varepsilon^2). \tag{3.42}$$

The normal flux $\hat{J}_n = \mathbf{n}\cdot\hat{\mathbf{J}}$ is given by

$$\hat{J}_n = \frac{M(U)}{\varepsilon}\partial_\rho\eta = \left[M'(-1)\hat{U}_1 + O(\varepsilon)\right]\left[\varepsilon\partial_y\hat{\eta}_1 + \varepsilon^2\partial_y\hat{\eta}_2 + O(\varepsilon^3)\right]. \tag{3.43}$$

Comparison with (3.41b) immediately implies $\hat{J}_{n,0} = 0$.

Leading order problem. To leading order, we have

$$-\partial_y \left[M'(-1)\hat{U}_1 \partial_y \hat{\eta}_1 \right] = 0, \tag{3.44a}$$

$$-\partial_{yy}\hat{U}_1 + f''(-1)\hat{U}_1 = \hat{\eta}_1. \tag{3.44b}$$

Integrating (3.44a) once, the expression in square brackets has to be a constant in y. From (3.43), we see this as the term $\hat{J}_{n,1}$ in the normal flux, which has to match to $J_{n,1}$ and $\mathbf{n}\cdot\mathbf{j}_1$ in the interface layer and the outer problem, respectively. Thus

$$\hat{J}_{n,1} = 0. \tag{3.45}$$

Therefore, the contribution $\hat{\eta}_1$ is also a constant that needs to match to the same value $\kappa/6$ towards the outer and the interface layer, i.e. for $\hat{y} \to \pm\infty$, so that we have

$$\hat{\eta}_1 = \frac{2}{3}\kappa \tag{3.46}$$

and

$$\hat{U}_1 = c_1 \mathrm{e}^{-2\mathrm{y}} + \mathrm{c}_2 \mathrm{e}^{2\mathrm{y}} + \frac{1}{6}\kappa. \tag{3.47}$$

Matching this to the constant outer $u_1 = \kappa/6$, obtained from (3.17) and (3.20), forces $c_2 = 0$. We next expand U_0 at $\rho \to \infty$,

$$U_0 = -1 + 2\mathrm{e}^{-2\rho} + \mathrm{O}(\mathrm{e}^{-4\rho}). \tag{3.48}$$

The second term accrues a factor of ε upon passing to y-variables, and thus has to match with the exponential term in $\varepsilon\hat{U}_1$, giving $c_1 = 2$ and

$$\hat{U}_1 = 2\mathrm{e}^{-2\mathrm{y}} + \frac{1}{6}\kappa. \tag{3.49}$$

First correction problem. To next order, we obtain

$$-\partial_y \left[M'(-1)\hat{U}_1 \partial_y \hat{\eta}_2 \right] = 0, \tag{3.50a}$$

$$-\partial_{yy}\hat{U}_2 - \kappa\partial_y\hat{U}_1 + f''(-1)\hat{U}_2 + f'''(-1)\hat{U}_1 = \hat{\eta}_2, \tag{3.50b}$$

$$\hat{J}_{n,2} = M'(-1)\hat{U}_1 \partial_y \hat{\eta}_2. \tag{3.50c}$$

From (3.50a) and (3.50c), and matching the flux contribution $\hat{J}_{n,2}$to the outer $\mathbf{n}\cdot\mathbf{j}_2$, we obtain

$$M'(-1)\hat{U}_1 \partial_y \hat{\eta}_2 = \frac{1}{2}\, \mu_1 \nabla_n \mu_1|_\zeta \,, \tag{3.51}$$

which in turn has the solution

$$\hat{\eta}_2 = \frac{\mu_1 \nabla_n \mu_1|_\zeta}{\kappa M'(-1)} \ln\left(\frac{\kappa}{12}\mathrm{e}^{2\mathrm{y}} + 1 \right) + \frac{\kappa^2}{36}. \tag{3.52}$$

The integration constant has been fixed by matching $\hat{\eta}_2$ for $y \to -\infty$ with the interface solution η_2, see (3.27). We now need to check if the exponential term in (3.52) matches

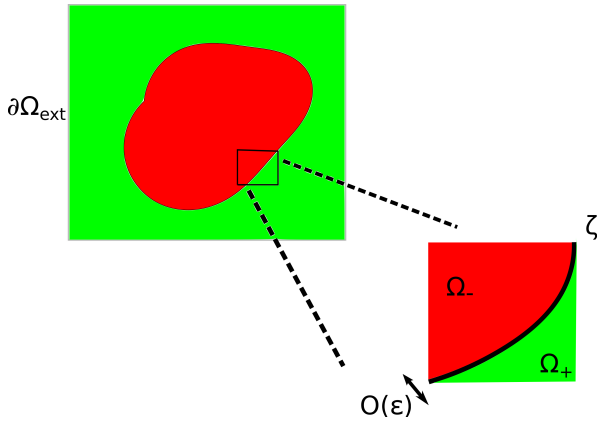

FIGURE 4.1. *The asymptotic structure of the sharp interface limit starting from initial conditions that are not bounded between* ± 1. *The solution consists of an interior layer near the interface separating two outer solutions.*

with the exponential term in (3.33). Expanding at $y \to -\infty$ is trivial, and then substituting in $y = \rho + \ln \varepsilon/2$ gives

$$\hat{\eta}_2 = \frac{\varepsilon}{8M'(-1)}\, \mu_1 \nabla_n \mu_1 \big|_\zeta \, \mathrm{e}^{2\rho} + \frac{\kappa^2}{36}. \tag{3.53}$$

Thus, $\varepsilon^2 \hat{\eta}_2$ contains a term proportional to $\varepsilon^3 \mathrm{e}^{2y}$ term that is identical to the $\varepsilon^3 \mathrm{e}^{2y}$ term that appears in $\varepsilon^3 \eta_3$, see (3.33). Thus, we have closed the matching and in particular resolved the issue of the exponentially growing term (for $\rho \to \infty$) in the interface layer correction for the chemical potential.

4. Modifications.

4.1. Non-bounds preserving solution. As pointed out in section 2, for initial conditions for u that violate the bound $u < 1$ inside the precipitate, the solution of the phase field model may evolve close to the equilibrium state given by the solution of (2.2) on the entire domain and with (2.2c) replaced by (2.3). We may therefore consider seeking the limiting sharp interface model for this case. The salient difference is that rather than having a contact line (arising from an exceedingly thin precursor), its asymptotic structure consists of an inner layer near the interface separating two outer solutions, see Fig. 4.1.

Following the argument outlined in section 3.3, we have

$$U_0 = -\tanh \rho, \tag{4.1}$$

for the inner solution, and constant outer solutions

$$u_0^{\pm} = \mp 1, \quad \mu_0^{\pm} = 0. \tag{4.2}$$

To next order, the inner expansion for the chemical potential reads

$$\partial_\rho (M(U_0) \partial_\rho \tilde{\mu}_1) = 0 \implies \tilde{\mu}_1 = \eta_1(s, \tau), \tag{4.3}$$

and for the order parameter

$$(f''(U_0) - \partial_{\rho\rho}) U_1 = \mu_1 + \kappa \partial_\rho U_0. \tag{4.4}$$

ε	0.01	0.005	0.002	0.001	**Eq (4.11)**
σ	-144.7	-146.3	-147.5	-147.8	$\mathbf{-148.1}$

TABLE 4.1

The decay rates of an azimuthal perturbation obtained by the diffuse and sharp interface models show good agreement for general initial condition not bounded between ± 1 and mobility $M(u) = 1 - u^2$. The numerical method and discretisation parameters are the same as in Table 3.1. The description of the numerical approach and parameters carries over from Table 3.1.

Now we require the inner solution to match to the outer solution inside the precipitate at $\rho \to -\infty$ and for $\rho \to \infty$ to the outer solution outside the precipitate. Imposing the solvability condition results in the same leading order contribution to the chemical potential and for U_1 as in section 3,

$$\mu_1 = \frac{2\kappa}{3}, \qquad U_1 = \frac{\kappa}{6}\tanh^2\rho. \tag{4.5}$$

Moreover, for the outer correction to $O(\varepsilon)$, we have

$$\nabla\cdot\left(M'(u_0^\pm)u_1^\pm\nabla\mu_0^\pm\right) + \nabla\cdot\left(M(u_0^\pm)\nabla\mu_1^\pm\right) = 0 \implies \mu_1^\pm = f''(u_0^\pm)u_1^\pm = 4u_1^\pm. \tag{4.6}$$

To $O(\varepsilon^2)$, it suffices to note from equation (3.25) that μ_2 is constant in ρ. The outer expansion reads

$$\nabla\cdot\left(M'(u_0^\pm)u_1^\pm\nabla\mu_1^\pm\right) = 0 \implies \nabla\cdot(\mu_1^\pm\nabla\mu_1^\pm) = 0, \tag{4.7}$$

with the no-flux boundary condition $\nabla_n\mu_1^\pm = 0$ on $\partial\Omega_{\text{ext}}$ and the matching condition $\mu_1^\pm = 2\kappa/3$ on ζ.

Equation (3.28) relates the interfacial velocity to the flux, *viz.*

$$v_n = \frac{1}{2}\left[M(U_0)\partial_\rho\mu_3\right]_{-\infty}^{\infty} + \frac{2}{3}\partial_{ss}\kappa. \tag{4.8}$$

Matching the fluxes, we have

$$\lim_{\rho\to\pm\infty} M(U_0)\partial_\rho\mu_3 = -\frac{1}{2}\mu_1^\pm\nabla_n\mu_1^\pm|_\zeta. \tag{4.9}$$

Hence, all in all, the sharp interface limit is the solid diffusion model coupled with a steady porous medium equation on both sides of the interface:

$$\begin{aligned} v_n &= \frac{2}{3}\partial_{ss}\kappa + \frac{1}{4}(\mu_1^+\nabla_n\mu_1^+ + \mu_1^-\nabla_n\mu_1^-), \text{ on } \zeta,\\ \nabla\cdot(\mu_1^\pm\nabla\mu_1^\pm) &= 0, \text{ on } \Omega_\pm,\\ \mu_1^\pm &= \frac{2}{3}\kappa, \text{ on } \zeta,\\ \nabla_n\mu_1^+ &= 0, \text{ on } \partial\Omega_{\text{ext}}. \end{aligned} \tag{4.10}$$

This sharp interface model predicts an exponential decay rate of

$$\sigma = -\frac{2}{3}\frac{m^2(m^2-1)}{r_0^4} - \frac{1}{9}\frac{m(m^2-1)}{r_0^4}(\tanh(m\log r_0^{-1}) + 1) \tag{4.11}$$

for an azimuthal perturbation to the axisymmetric stationary state with curvature $1/r_0$. Table 4.1 shows that equation (4.11) is indeed consistent with numerical results,

ε	0.01	0.005	0.001	**Eq (3.35)**
σ	-84.6	-84.7	-85.2	-85.$\dot{3}$

TABLE 4.2

The decay rates obtained by the diffuse interface model for the mobility $M(u) = (1-u^2)^2$ and $|u| < 1$ show good agreement with the solid diffusion model in (3.35)*, with $\mathfrak{M} = 4/9$, as $\varepsilon \to 0$. The description of the numerical approach and parameters carries over from table* (3.1).

confirming that the sharp interface limit reduces to the two-sided porous medium model (4.10) if the initial condition is not bounded between the pure phases.

As a cautionary remark, we note that we are dealing here with a sign-changing solution of a degenerate fourth order problem (in the sense that $1-u$ changes sign and the mobility degenerates). The theory for these type of problems is still being developed [29, 28, 4, 15, 11, 30]. It is not clear a-priori if a unique solution exists, but our results suggest that the evolution approximated by the numerical solution of the phase field model agrees with the sharp interface model obtained from the asymptotic derivations.

4.2. Doubly degenerate mobility. For the mobility $M_1(u) = 1-u^2$ investigated so far, the nonlinear bulk diffusion enters at the same order as surface diffusion. If we employ a mobility function such that $M(\pm 1) = M'(\pm 1) = 0$, such as $M(u) = (1-u^2)^2$, then

$$j_2 = u_1 M'(u_0) \nabla_n \mu_1 = 0. \tag{4.12}$$

The contribution of the bulk diffusion flux to the normal velocity of the interface is subdominant to surface diffusion and therefore

$$v_n = \frac{1}{3} \int_{-\infty}^{\infty} \operatorname{sech}^4 \rho \, \mathrm{d}\rho \, \partial_{ss} \kappa = \frac{4}{9} \partial_{ss} \kappa. \tag{4.13}$$

Table 4.2 shows that the decay rate of an azimuthal perturbation obtained by propagating the diffuse interface model for $M(u) = (1-u^2)^2$, obtained here for the bounds preserving solution, is indeed consistent with the pure solid diffusion model.

5. Conclusions. In this paper, we have derived the sharp interface limit for a Cahn–Hilliard model with a nonlinear mobility that has a simple zero if the order parameter is ± 1, and a smooth, polynomial double-well potential with minima at ± 1 for the homogeneous part of the free energy. We found that in addition to surface diffusion, there is also bulk diffusion contributing to the interface motion at the same order. Depending on the initial data, which can be close to an equilibrium state that respects the bounds $|u| < 1$, or to one that does not, the bulk diffusion acts from one side of the interface, or from both.

The situation studied here was focused on a single precipitate, though the asymptotic analysis remains valid for any collection of closed convex domains. The derivation does, however, tacitly assume that the curvature of the interface is $O(1)$. For the case where the interface has turning points, the derivation needs to be revisited, since for the bounds-preserving phase field for example, the contact line is expected to change from one side to the other and cross the interface. The dynamics in more complex geometries such as, for example, concentric circles of different phases are likely to be more subtle; reflections on this issue can be found in [50]. On a different plane, it would also be interesting to investigate the coarsening behaviour [17] for the sharp

interface model (3.34). For a pair or larger ensembles of disconnected spheres, pure surface diffusion does not give rise to coarsening, but is expected for (3.34), due to the leading order contribution of the nonlinear porous medium like bulk diffusion to v_n, see (3.34d).

While the specific Cahn–Hilliard equation we focused on here plays a role in some biological models, see for example [46], and may have significance in modelling spinodal decomposition in porous media, possibly with different combinations of mobilities, e.g. $M(u) = |1 - u^2| + \alpha(1 - u^2)^2$, see [50], the main motiviation for our investigation stems from the interest to use phase field models as a basis for numerical codes for surface diffusion simulations. The bottom line is of course that the combination of the mobility M_1 and free energy f_p is not useful for this purpose, since there always is a contribution from bulk diffusion that cannot be mitigated by reducing ε. For mobilities with higher degeneracy, this undesired effect is of smaller order, e.g. we expect it to be $O(\varepsilon)$ if M_1 is replaced by M_2, which is also supported by our numerical results. Nevertheless, it is still present, and can accumulate over time, leading for example to a small but persistent coarsening effect. Therefore, to obtain reliable and accurate results, the time period over which a simulation is to be conducted places an upper bound on the acceptable choice of ε.

Moreover, higher order degeneracies can have other undesirable effects. In thin film settings, where degenerate fourth order PDE models play an important role [24, 56], mobilities with a degeneracy equal to or higher than three may introduce singularities that impede the motion of the contact line see [12, 44] and literature cited in [13] and the previously mentioned reviews. As a result, the solutions could in principle depend on the explicit or implicit regularisation, e.g. on the precursor thickness or the details of the numerical discretisation. It is unclear how, in the context of Cahn–Hilliard models, this dependence would affect the motion of the interface for the bounds-preserving phase field model and even less so if the order parameter is permitted to leave the interval $[-1, 1]$. A documentation of the initial condition for and a monitoring of the behaviour of the order parameter for simulations using phase field models with degenerate mobilities is desirable in any case.

An alternative is to resort to the combination of M_1 with the free energy f_l, or a double obstacle potential, since these seem to force the order parameter to be equal to or much closer to the ± 1, thus shutting out the bulk diffusion more effectively. The more singular nature of these potentials seems to be awkward to handle numerically, but successful approaches that preserve the bounds on the order parameter have been reported and analysed in the literature, see for example [6, 9, 7, 8, 10, 31, 5]. Other approaches that have been suggested include a dependence of the mobility on the gradients of the order parameter [53], tensorial mobilities [38], or more singular expressions for the flux [61]. However, for any approach, a careful asymptotic analsysis has to ensure that in the sharp interface limit $\varepsilon \to 0$, bulk diffusion is either absent or sufficiently small. In particular, in situations where the suppression of bulk diffusion hinges on the outer solution for the order parameter being equal to ± 1, this property cannot simply be assumed a-priori, but has to be consistent with a comprehensive asymptotic analysis of the limit $\varepsilon \to 0$.

6. Appendix: Numerical Methods. We solved the fourth order PDE numerically via Chebyshev spectral collocation method for spatial discretisation and semi-implicit time-stepping. For further details on spectral methods we refer the reader to Refs [66, 67].

To summarise, denoting $\mathbf{u}^n = [u_0^n, u_1^n, \ldots, u_{N+1}^n]$ and $\boldsymbol{\mu}^n = [\mu_0^n, \mu_1^n, \ldots, \mu_{N+1}^n]$,

where u_i^n is the numerical approximation to $u(r_i, t_n)$ and μ_i^n is the numerical approximation to $\mu(r_n, t_n)$ with $t_n = n\Delta t$ and r_n the position of the n^{th} mesh point, our semi-implicit scheme reads

$$\frac{\mathbf{u}^{n+1} - \mathbf{u}^n}{\Delta t} = \mathcal{L}\boldsymbol{\mu}^{n+1} + \theta\tilde{\Delta}(\boldsymbol{\mu}^{n+1} - \boldsymbol{\mu}^n), \tag{6.1}$$

$$\boldsymbol{\mu}^{n+1} = -\varepsilon^2\tilde{\Delta}\mathbf{u}^{n+1} + \mathbf{f}'(\mathbf{u}^n) + \mathrm{diag}(\mathbf{f}''(\mathbf{u}^n))(\mathbf{u}^{n+1} - \mathbf{u}^n), \tag{6.2}$$

where $\tilde{\Delta}$ denotes the approximation to the Laplacian via the collocation method. A linearised convex splitting scheme has been used to treat the free energy, and we split the mobility as $M(u) \equiv (M(u) - \theta) + \theta$, to evaluate $(M(u) - \theta)$ at the previous time step whilst solving the remaining θ portion at the next time step. This is to ameliorate the stringent time-stepping constrains. Numerical experiments indicate that the results are not sensitive to precise values of θ as long as $\theta = O(\varepsilon)$, and we choose $\theta = 0.01\varepsilon$.

For the axisymmetric case,

$$\tilde{\Delta} = D^2 + \mathrm{diag}(1/\boldsymbol{x})D, \tag{6.3}$$

where D is the differentiation matrix, and $\boldsymbol{x}$ denotes the vector of Chebyshev–Lobatto collocation points ($x_j = \cos(\pi j/N)$, where N is the number of mesh points). As the Chebyshev–Lobatto points are scarcest in the middle of the domain, we resolve the interior layer by introducing a non-linear map to the Chebyshev-Lobatto points that maps $x \in [-1, 1] \mapsto r \in [0, 1]$, as suggested in [16],

$$r = \frac{1}{2} + \frac{1}{\pi}\mathrm{arctan}\left(\delta \tan\frac{\pi}{2}x\right), \tag{6.4}$$

where $0 < \delta < 1$ is a parameter that determines the degree of stretching of the interior domain, with a smaller value of δ corresponding to greater degree of localisation of mesh points about the centre of the domain. The differential equation can be readily transformed by recalling the chain rule

$$\frac{\mathrm{d}}{\mathrm{d}r}f(r(x)) = \frac{\mathrm{d}x}{\mathrm{d}r}\frac{\mathrm{d}f}{\mathrm{d}x}. \tag{6.5}$$

After some algebra we have

$$\begin{aligned} f_r &= \frac{1}{\delta}(1 + \delta^2 - (\delta^2 - 1)\cos\pi x)f_x, \\ f_{rr} &= \frac{1}{\delta^2}(1 + \delta^2 - (\delta^2 - 1)\cos\pi x)^2 f_{xx} \\ &\quad -\frac{1}{\delta^2}(\delta^4 - 1 - (\delta^2 - 1)^2\cos\pi x)\pi\sin\pi x f_x. \end{aligned} \tag{6.6}$$

Thus the differentiation matrices can be scaled according to equation (6.6). In this paper, the modified collocation method is used with $\delta = 10\varepsilon$. This choice of δ is guided by numerical experiments, which show that further increase in the number of mesh points does not alter the stationary solution. The point $x = 0$ is a regular singular point, and to avoid numerical divergences we map the domain $r \in [0, 1] \mapsto [\alpha, 1]$ with

$\alpha = 10^{-10}$ via a linear transformation, the choice of any smaller α does not affect the numerical results.

Unless otherwise stated, the numerical simulations reported in the paper are done with 400 collocation points and timestep $\Delta t = 10^{-3}$. We note that our numerical scheme using semi-implicit time stepping with linearised convex-spliting on the free energy is bound-preserving as long as the initial data takes value between $[-1, 1]$, the time steps are sufficiently small, and the spatial discretisation allows resolution of the interior layer. No truncation or "push-back" of values that exceeded ± 1 is required.

REFERENCES

[1] H. Abels and M. Röger, *Existence of weak solutions for a non-classical sharp interface model for a two-phase flow of viscous, incompressible fluids*, Annales de l'Institut Henri Poincare (C) Non Linear Analysis, 26 (2009), pp. 2403–2424.

[2] N. D. Alikakos, P. W. Bates, and X. Chen, *Convergence of the Cahn-Hilliard equation to the Hele-Shaw model*, Archive for Rational Mechanics and Analysis, 128 (1994), pp. 165–205.

[3] R. F. Almgren, *Second-order phase field asymptotics for unequal conductivities*, SIAM Journal on Applied Mathematics, 59 (1999), pp. 2086–2107.

[4] P. Alvarez-Caudevilla and V. A. Galaktionov, *Well-posedness of the cauchy problem for a fourth-order thin film equation via regularization approaches*, arXiv:1311.0712 [math], (2013).

[5] L. Banaš, A. Novick-Cohen, and R. Nüernberg, *The degenerate and non-degenerate deep quench obstacle problem: A numerical comparison*, Networks and Heterogeneous Media, 8 (2013), pp. 37–64.

[6] J. W. Barrett and J. F. Blowey, *Finite element approximation of a degenerate Allen–Cahn/Cahn–Hilliard system*, SIAM Journal on Numerical Analysis, 39 (2002), pp. 1598–1624.

[7] J. W. Barrett, J. F. Blowey, and H. Garcke, *Finite element approximation of a fourth order nonlinear degenerate parabolic equation*, Numerische Mathematik, 80 (1998), pp. 525–556.

[8] ———, *Finite element approximation of the Cahn–Hilliard equation with degenerate mobility*, SIAM Journal on Numerical Analysis, 37 (1999), pp. 286–318.

[9] ———, *On fully practical finite element approximations of degenerate Cahn-Hilliard systems*, ESAIM: Mathematical Modelling and Numerical Analysis, 35 (2002), pp. 713–748.

[10] J. W. Barrett, H. Garcke, and R. Nürnberg, *A phase field model for the electromigration of intergranular voids*, Interfaces and Free Boundaries, 9 (2007), p. 171–210.

[11] F. Bernis, *Finite speed of propagation and continuity of the interface for thin viscous flows*, Advances in Differential Equations, 1 (1996), pp. 337–368.

[12] F. Bernis and A. Friedman, *Higher order nonlinear degenerate parabolic equations*, Journal of Differential Equations, 83 (1990), pp. 179–206.

[13] A. Bertozzi, *The mathematics of moving contact lines in thin liquid films*, Notices AMS, 45 (1998), p. 689–697.

[14] D. N. Bhate, A. Kumar, and A. F. Bower, *Diffuse interface model for electromigration and stress voiding*, Journal of Applied Physics, 87 (2000), pp. 1712–1721.

[15] M. Bowen and T. P. Witelski, *The linear limit of the dipole problem for the thin film equation*, SIAM Journal on Applied Mathematics, 66 (2006), pp. 1727–1748.

[16] J. P Boyd, *The arctan/tan and Kepler-Burgers mappings for periodic solutions with a shock, front, or internal boundary layer*, Journal of Computational Physics, 98 (1992), pp. 181–193.

[17] A. J. Bray and C. L. Emmott, *Lifshitz-Slyozov scaling for late-stage coarsening with an order-parameter-dependent mobility*, Physical Review B, 52 (1995), pp. R685–R688.

[18] J. W. Cahn and J. E. Hilliard, *Spinodal decomposition: A reprise*, Acta Metallurgica, 19 (1971), pp. 151–161.

[19] J. W. Cahn and J. E. Taylor, *Surface motion by surface diffusion*, Acta Metallurgica et Materialia, 42 (1994), pp. 1045–1063.

[20] J. W. Cahn, C. M. Elliott, and A. Novick-Cohen, *The Cahn-Hilliard equation with a concentration dependent mobility: motion by minus the laplacian of the mean curvature*, European Journal of Applied Mathematics, 7 (1996), pp. 287–302.

[21] J. W. Cahn and J. E. Hilliard, *Free energy of a nonuniform system. i. interfacial free energy*, The Journal of Chemical Physics, 28 (1958), p. 258.
[22] H. D. Ceniceros and C. J. García-Cervera, *A new approach for the numerical solution of diffusion equations with variable and degenerate mobility*, Journal of Computational Physics, (2013).
[23] L. Chen, *Phase-field models for microstructure evolution*, Annual review of materials research, 32 (2002), pp. 113–140.
[24] R. V. Craster and O. K. Matar, *Dynamics and stability of thin liquid films*, Reviews of Modern Physics, 81 (2009), pp. 1131–68.
[25] S. Dai and Q. Du, *Motion of interfaces governed by the Cahn–Hilliard Equation with highly disparate diffusion mobility*, SIAM Journal on Applied Mathematics, 72 (2012), pp. 1818–1841.
[26] R. Dal Passo, H. Garcke, and G. Grün, *On a fourth-order degenerate parabolic equation: Global entropy estimates, existence, and qualitative behavior of solutions*, SIAM Journal on Mathematical Analysis, 29 (1998), pp. 321–342.
[27] C. M. Elliott and H. Garcke, *On the Cahn-Hilliard equation with degenerate mobility*, SIAM Journal on Mathematical Analysis, 27 (1996), pp. 404–423.
[28] J. D. Evans, V. A. Galaktionov, and J. R. King, *Source-type solutions of the fourth-order unstable thin film equation*, European Journal of Applied Mathematics, 18 (2007), pp. 273–321.
[29] V. A. Galaktionov, *Very singular solutions for thin film equations with absorption*, Studies in Applied Mathematics, 124 (2010), p. 39–63.
[30] ———, *On oscillations of solutions of the fourth-order thin film equation near heteroclinic bifurcation point*, (2013).
[31] H. Garcke, R. Nürnberg, and V. Styles, *Stress- and diffusion-induced interface motion: Modelling and numerical simulations*, European Journal of Applied Mathematics, 18 (2007), pp. 631–657.
[32] G. Giacomin and J. L Lebowitz, *Exact macroscopic description of phase segregation in model alloys with long range interactions*, Physical Review Letters, 76 (1996), p. 1094.
[33] ———, *Phase segregation dynamics in particle systems with long range interactions I: Macroscopic limits*, Journal of Statistical Physics, 87 (1997), pp. 37–61.
[34] ———, *Phase segregation dynamics in particle systems with long range interactions II: Interface motion*, SIAM Journal on Applied Mathematics, 58 (1998), pp. 1707–1729.
[35] G. Giacomin, J. L. Lebowitz, and R. Marra, *Macroscopic evolution of particle systems with short-and long-range interactions*, Nonlinearity, 13 (2000), p. 2143.
[36] K. Glasner, *A diffuse interface approach to Hele–Shaw flow*, Nonlinearity, 16 (2003), p. 49.
[37] G. Grün and M. Rumpf, *Nonnegativity preserving convergent schemes for the thin film equation*, Numerische Mathematik, 87 (2000), pp. 113–152.
[38] C. Gugenberger, R. Spatschek, and K. Kassner, *Comparison of phase-field models for surface diffusion*, Physical Review E, 78 (2008), p. 016703.
[39] Mark H Holmes, *Introduction to perturbation methods*, vol. 20, Springer, 2013.
[40] W. Jiang, W. Bao, C. V. Thompson, and D. J. Srolovitz, *Phase field approach for simulating solid-state dewetting problems*, Acta Materialia, 60 (2012), pp. 5578–5592.
[41] A. Karma and W. Rappel, *Phase-field method for computationally efficient modeling of solidification with arbitrary interface kinetics*, Physical Review E, 53 (1996), p. R3017.
[42] ———, *Quantitative phase-field modeling of dendritic growth in two and three dimensions*, Physical Review E, 57 (1998), p. 4323.
[43] J. Kevorkian and J. D. Cole, *Multiple scale and singular perturbation methods*, vol. 114, Springer New York, 1996.
[44] J. R. King and M. Bowen, *Moving boundary problems and non-uniqueness for the thin film equation*, European Journal of Applied Mathematics, 12 (2001), pp. 321–356.
[45] K. Kitahara and M. Imada, *On the kinetic equations for binary mixtures*, Progress in Theoretical Physics Suppliment, 64 (1978), pp. 65–73.
[46] I. Klapper and J. Dockery, *Role of cohesion in the material description of biofilms*, Physical Review E, 74 (2006).
[47] R. V. Kohn and F. Otto, *Upper bounds on coarsening rates*, Communications in Mathematical Physics, 229 (2002), pp. 375–395.
[48] M. D. Korzec, P. L. Evans, A. Münch, and B. Wagner, *Stationary solutions of driven fourth-and sixth-order Cahn-Hilliard-type equations*, SIAM Journal on Applied Mathematics, 69 (2008), pp. 348–374.
[49] C. G. Lange, *On spurious solutions of singular perturbation problems*, Studies in Applied Mathematics, 68 (1983), pp. 227–257.

[50] A. A. Lee, *On the Sharp Interface Limits of the Cahn-Hilliard Equation*, M.Sc. thesis, University of Oxford, 2013.
[51] P. Loreti and R. March, *Propagation of fronts in a nonlinear fourth order equation*, European Journal of Applied Mathematics, 11 (2000), pp. 203–213.
[52] H.-W. Lu, K. Glasner, A. L. Bertozzi, and C.-J. Kim, *A diffuse-interface model for electrowetting drops in a hele-shaw cell*, Journal of Fluid Mechanics, 590 (2007), pp. 411–435.
[53] M. Mahadevan and R. M. Bradley, *Phase field model of surface electromigration in single crystal metal thin films*, Physica D: Nonlinear Phenomena, 126 (1999), pp. 201–213.
[54] W. W. Mullins and R. F. Sekerka, *Morphological stability of a particle growing by diffusion or heat flow*, Journal of Applied Physics, 34 (1963), pp. 323–329.
[55] A. Novick-Cohen, *The Cahn-Hilliard equation*, Handbook of differential equations: evolutionary equations, 4 (2008), pp. 201–228.
[56] A. Oron, S. H. Davis, and S. G. Bankoff, *Long-scale evolution of thin liquid films*, Reviews of Modern Physics, 69 (1997), p. 931.
[57] R. L. Pego, *Front migration in the nonlinear Cahn-Hilliard equation*, Proceedings of the Royal Society of London. A. Mathematical and Physical Sciences, 422 (1989), pp. 261–278.
[58] N. Provatas and K. Elder, *Phase-field methods in materials science and engineering*, Wiley Interscience, 2010.
[59] S. Puri, A. J. Bray, and J. L. Lebowitz, *Phase-separation kinetics in a model with order-parameter-dependent mobility*, Physical Review E, 56 (1997), pp. 758–765.
[60] A. Rätz, A. Ribalta, and A. Voigt, *Surface evolution of elastically stressed films under deposition by a diffuse interface model*, Journal of Computational Physics, 214 (2006), pp. 187–208.
[61] ———, *Surface evolution of elastically stressed films under deposition by a diffuse interface model*, Journal of Computational Physics, 214 (2006), pp. 187–208.
[62] D. N. Sibley, A. Nold, and S. Kalliadasis, *Unifying binary fluid diffuse-interface models in the sharp-interface limit*, Journal of Fluid Mechanics, 736 (2013), pp. 5–43.
[63] J. E. Taylor and J. W. Cahn, *Linking anisotropic sharp and diffuse surface motion laws via gradient flows*, Journal of Statistical Physics, 77 (1994), pp. 183–197.
[64] S. Torabi and J. Lowengrub, *Simulating interfacial anisotropy in thin-film growth using an extended cahn-hilliard model*, Physical Review E, 85 (2012), p. 041603.
[65] S. Torabi, J. Lowengrub, A. Voigt, and S. Wise, *A new phase-field model for strongly anisotropic systems*, Proceedings of the Royal Society A: Mathematical, Physical and Engineering Science, 465 (2009), pp. 1337–1359.
[66] L. N. Trefethen, *Spectral methods in MATLAB*, vol. 10, SIAM, 2000.
[67] L. N Trefethen, *Approximation theory and approximation practice*, SIAM, 2013.
[68] S. van Gemmert, G. T. Barkema, and S. Puri, *Phase separation driven by surface diffusion: A monte carlo study*, Physical Review E, 72 (2005), p. 046131.
[69] J. K. Wolterink, G. T. Barkema, and S. Puri, *Spinodal decomposition via surface diffusion in polymer mixtures*, Physical Review E, 74 (2006), p. 011804.
[70] L. Zhornitskaya and A. L. Bertozzi, *Positivity-preserving numerical schemes for lubrication-type equations*, SIAM Journal on Numerical Analysis, 37 (2000), pp. 523–555.